Nature Microbiology. Letter

Origins of pandemic *Vibrio cholerae* from environmental gene pools

B. Jesse Shapiro[1], Inès Levade[1#], Gabriela Kovacikova[2#], Ronald K. Taylor[2‡], Salvador Almagro-Moreno[2,3]*

[1]Department of Biological Sciences, University of Montreal, Montreal, Quebec, Canada. [2]Department of Microbiology and Immunology, Geisel School of Medicine at Dartmouth, Hanover, New Hampshire, USA. [3]Burnett School of Biomedical Sciences, College of Medicine, University of Central Florida, Orlando, Florida, USA.

*For correspondence: samoreno@ucf.edu

[#]These authors contributed equally

[‡]Deceased

Abstract

Some microbes can transition from an environmental lifestyle to a pathogenic one[1-3]. This ecological switch typically occurs through the acquisition of horizontally acquired virulence genes[4,5]. However, the genomic features that must be present in a population prior to the acquisition of virulence genes and emergence of pathogenic clones remain unknown. We hypothesized that virulence adaptive polymorphisms (VAPs) circulate in environmental populations and are required for this transition. We developed a comparative genomic framework for identifying VAPs, using *Vibrio cholerae* as a model. We then characterized several environmental VAP alleles to show that, while some of them reduced the ability of clinical strains to colonize a mammalian host, other alleles conferred efficient host colonization. These results show that VAPs are present in environmental bacterial populations prior to the emergence of virulent clones. We propose a scenario in which VAPs circulate in the environment, they become selected and enriched under certain ecological conditions, and finally a genomic background containing several VAPs acquires virulence factors that allows for its emergence as a pathogenic clone.

Main text

Numerous bacterial pathogens have emerged from environmental populations[1-3,6]. These virulent clones evolve through the acquisition of toxins and host colonization factors[4,5]. Given that the genes encoding these factors can often spread widely by horizontal gene transfer, it is surprising that only a limited number of pathogenic clones have emerged from any particular bacterial species. As a model of how environmental gene pools give rise to pandemic clones, we used *Vibrio cholerae*, a genetically diverse group of aquatic bacteria that include a confined phylogenetic group, the "pandemic genome" group (PG), that can cause the severe diarrheal disease cholera in humans[7,8]. Seven pandemics of cholera have been recorded to date, all caused by the PG group. The current pandemic is caused by strains of the El Tor biotype, and has spread across the globe in several waves of transmission[9]. Virulence in *V. cholerae* PG is mainly determined by two virulence factors: the cholera toxin (CT) and the toxin-coregulated pilus (TCP), which are encoded within horizontally acquired genetic elements, the CTXΦ phage and the Vibrio Pathogenicity Island-1 (VPI-1) respectively[10-12]. Both CTXΦ and VPI-1 are always found in the PG group, however, they are also encoded in some environmental populations of *V. cholerae*[13-15]. Furthermore, even though some non-PG strains can cause gastrointestinal infections, only strains from the PG clade have ever emerged as a source of pandemic cholera[16].

To investigate the evolutionary origins of pandemic clones of *V. cholerae* and the potential for their reemergence, we analyzed 43 *V. cholerae* genomes sequenced from clinical and environmental samples (Methods; Supplementary Table 1). These genomes span the known genetic diversity of *V. cholerae* (Supplementary Notes), and were divided into a primary dataset of 22 genomes and a replication dataset of 22 genomes, with one reference genome in common (Supplementary Table 2). In the primary dataset, we chose 7 PGs, including both

54 classical strains, the source of the first six pandemics, and El Tor, to represent the genetic
55 diversity of the pandemic group. We compared these with 15 non-clinical environmental
56 genomes (EGs): 10 EGs from worldwide samples to include global diversity, and five sympatric
57 isolates from the Great Bay Estuary (GBE) in New Hampshire, USA, a region with no recent
58 history of cholera outbreaks[17].

59 Consistent with the results of previous studies[7,9,17,18], PGs form a distinct monophyletic
60 group compared to EGs, based on the aligned core genome (Fig. 1a). Other than the PG group,
61 there is little phylogenetic structure and the tree is star-like in both datasets (Supplementary Fig.
62 1). Reticulations in the phylogenetic network indicate recombination or homoplasies (repeated
63 mutations in independent lineages at the same locus), consistent with a large, genetically
64 diverse and recombining *V. cholerae* population[18,19] (Supplementary Fig. 1). Given such a
65 recombining population with mobile virulence factors, it remains puzzling why the ability to
66 cause pandemic cholera is limited to the PG group.

67 To find unique features of PGs that could explain their pandemic success, we first
68 searched for genes present in PGs but absent in EGs. Although there are a few genes and
69 gene clusters which appear to be universally present in PGs, including CTXΦ and VPI-1, none
70 of these are unique to PGs as they are also present in some EGs (Supplementary Table 3).
71 This observation is consistent with previous work showing that these virulence genes are rapidly
72 gained and lost in both EGs and PGs[7,18]. Therefore, there appear to be no gene families whose
73 presence can easily explain the origin of pandemic cholera, nor are there strong boundaries to
74 gene transfer between PGs and EGs.

75 Given the lack of PG-specific genes, we hypothesized that the environmental ancestor of
76 the PGs had a particular genomic background containing alleles of core genes – which we term
77 virulence adaptive polymorphisms (VAPs) – that served as “preadaptations” and enhanced its
78 potential to give rise to pandemic disease. We started our search for VAPs by identifying SNPs

in the aligned core of the 22 primary dataset genomes with one allele uniquely present in all PGs and a different allele uniquely present in all EGs. We called this a “fixed” SNP pattern. We identified 819 such fixed SNPs distributed across the genome (Fig. 1b; Supplementary Fig. 3). Some fixed SNPs could have contributed to the evolution of the pandemic phenotype in PG, while others could be selectively neutral hitchhikers on the PG genomic background. Using the McDonald-Kreitman test (Methods), we found evidence for genome-wide positive selection during the divergence of PGs from EGs, due to an excess of nonsynonymous changes at fixed sites, in both datasets (Supplementary Table 4). However, no individual gene showed evidence for selection after correcting for multiple tests (Methods), rendering it difficult to identify candidate VAPs using fixed SNPs. Nonetheless, fixed SNPs constitute only a modest fraction of possible SNP patterns (Supplementary Table 2), and VAPs could also exist at other SNP sites that might shed light in the evolutionary past of the ancestral PG.

We then defined and searched for a “mixed” SNP pattern, where PGs encode one fixed allele and EGs encode a “mix” of two alleles: one that is unique to EGs and also one that is fixed in PGs (Fig. 1c inset). We reasoned that the existence of PG-like alleles segregating in contemporary environmental populations of *V. cholerae* could be informative about: 1) pathogen emergence, because having an allele fixed in PG suggests that it could also have been present in the environmental ancestor of PG; and 2) the potential for pathogen reemergence, as PG-like alleles, and thus potential VAPs, are still circulating in the environmental gene pool. We identified 39,171 mixed SNPs in the primary dataset. Most genes contain few mixed SNPs (median of 3) but some genes contain dense clusters, resulting in a mean of 10.3 mixed SNPs per gene. The replication dataset contained greater genetic diversity, but showed the same pattern of a few genes containing many mixed SNPs (Supplementary Table 2). Clusters of genes containing many mixed SNPs are visible when plotted across the genome (Fig. 1c). Some of these clusters are known polymorphic regions of the genome and could be mutation

hotspots containing SNPs not directly relevant to virulence adaptation. However, clusters of mixed SNPs do not visibly overlap with clusters of overall polymorphism (Fig. 1c), indicating that accumulation of mixed SNPs cannot be explained only by mutation hotspots.

To formally exclude mutation hotspots and focus on clusters of mixed SNPs shaped mainly by natural selection instead of mutation and drift, we considered only genes with an excess of nonsynonymous (NS) mixed SNPs relative to synonymous (S) mixed SNPs, which control for the baseline mutation rate. The mixed SNP pattern by definition groups PG-like EGs away from the other environmental strains and clusters them with the PGs. We reasoned that genes with an elevated NS:S ratio at mixed SNP sites were more likely to show phenotypic variations and have evolved under positive selection, possibly underlying preadaptations of the PG ancestor. Using a threshold of the number of mixed NS SNPs, NS:S, and *dN/dS* all two standard deviations above their genome-wide medians (Methods), we identified five genes as candidate VAPs in the primary dataset, three of which survived multiple hypothesis correction, and two of which (*ompU* and hypothetical gene VCD_001600) were also found in the replication dataset (Table 1). In contrast to the star-like genome-wide phylogeny (Fig. 1a), each of these five gene trees support one or more EGs grouping with PGs (Fig. 1d and Supplementary Fig. 4). Three additional VAPs – all hypothetical proteins – were identified in the replication dataset, suggesting the potential for other candidate VAPs to be identified with further sampling of genetically diverse environmental genomes (Supplementary Table 5).

Among the candidate VAPs, the gene with the most significant excess of mixed nonsynonymous SNPs in both datasets is *ompU* (Table 1). OmpU is an outer membrane porin that has been shown to play numerous roles in the intestinal colonization of *V. cholerae*, making it a compelling candidate for phenotypic characterization[20-23]. We observed that environmental strains RC385, GBE0658 and GBE0428 have PG-like *ompU* alleles whereas most environmental strains, such as GBE1114, branch distantly from PG (Fig. 1d). We hypothesized

that the PG-like alleles present in environmental strains might confer properties conducive to virulence. To test this, we constructed three different mutant strains each encoding one of three environmental alleles of *ompU* (all from sympatric GBE strains) into the background of N16961, a clinical strain from the current pandemic (Fig. 2). OmpU was detected on a protein gel stained with Coomassie blue and through immunoblot in all the constructed strains, indicating that all the strains effectively produce the environmental versions of the protein (Fig. 2a and Supplementary Fig. 6). The band size differences reflect the diversity in protein sizes among the three environmental OmpU variants (Supplementary Fig. 5 and Supplementary Table 6).

We performed three sets of experiments to compare the phenotypes conferred by EG and PG-like alleles of *ompU*. First, we determined the survival of these strains in the presence of 0.4% bile, as it has been previously shown that OmpU confers resistance to this antimicrobial compound[20]. The mutant strain encoding the *ompU* allele from the environmental strain GBE1114 ($OmpU^{GBE1114}$) showed a similar survival rate in the presence of bile as a deletion mutant (Fig 2b). In contrast, $OmpU^{GBE0658}$ show similar survival in the presence of bile as a PG strain (Fig. 2b). These experiments indicate that some environmental alleles of *ompU* confer properties beneficial for virulence. Second, we tested the survival of the mutants in the presence of polymyxin B, as OmpU also confers resistance against this antibiotic[21]. The ability to tolerate the antimicrobial effects of polymyxin B appears to be independent of which *ompU* allele is encoded by *V. cholerae*, as the three strains encoding environmental alleles of *ompU* had a similar survival rate (Fig. 2c). This experiment shows that $OmpU^{GBE1114}$ is not simply a loss of function mutant, and is not equivalent to a knockout. Third, we determined the intestinal colonization of the *ompU* mutants by performing competition assays using the infant mouse model of human infection. We found that $OmpU^{GBE1114}$ had a colonization defect similar to Δ*ompU* whereas $OmpU^{GBE0658}$ was able to colonize similarly to the strain with the wild-type PG

153 allele (Fig. 2d). These results indicate that certain naturally occurring environmental alleles of
154 *ompU* confer properties that provide an advantage to *V. cholerae* during or prior to host
155 colonization, as would be expected for VAPs.

156 The *ompU*^{GBE1114} allele appears to be maladaptive for intestinal colonization; however, its
157 presence in several environmental isolates of *V. cholerae* prompted us to investigate its
158 possible adaptive role in the environment (Fig. 2e). *V. cholerae* forms biofilms on the surface of
159 biotic and abiotic environmental surfaces[24-26], yet biofilm formation inside the host is thought to
160 impair intestinal colonization[22,27]. Strains with deletions in *ompU* have been shown to form a
161 more robust biofilm on abiotic surfaces[25]. We found that OmpU^{GBE1114} has higher biofilm
162 formation than the strain encoding the wild-type PG allele, similar to the Δ*ompU* strain (Fig. 2e).
163 Both OmpU^{GBE0658} and OmpU^{GBE0428} formed biofilm similar to the strains with the wild-type PG
164 allele (Fig. 2e). It therefore appears that there is an evolutionary trade-off between encoding the
165 PG-like or EG-like alleles of VAPs, as they seem to confer mutually exclusive traits: either
166 biofilm formation or bile resistance and host colonization. This suggests that environmental
167 strains can be divided into subgroups which, due to their contrasting lifestyles, differ in their
168 potential to give rise to pandemic clones.

169 We have determined that virulence adaptive polymorphisms are present in the
170 environment, and shown how these VAPs can be identified, based on two independent sets of
171 genomes. The top candidate VAP, *ompU*, was identified in both of our genomic datasets. Our
172 experiments show that the *ompU* allele from some environmental strains, such as GBE0658,
173 confers properties that allow for host colonization equally as efficient as alleles from clinical
174 strains (Fig. 2). This leads to a natural question: Why have environmental strains with PG-like
175 alleles not emerged as pandemic cholera strains? It appears that a variety of virulence adaptive

genes and alleles are circulating in the environment, but only the PG group encodes the optimal combination of VAPs that allowed for pandemic potential (Fig. 3). We propose a conceptual model in which VAPs circulate in a diverse, recombining environmental gene pool, being maintained in the population through various biotic and abiotic selective pressures (Fig. 3a). A new ecological opportunity occurs, such as human consumption of brackish water or transient colonization of other animal hosts, which leads to the proliferation and gradual enrichment in the population of clones encoding a mosaic of VAPs (Fig. 3b). Finally, a genome encoding a critical combination of VAPs acquires key virulence factors allowing it to emerge as a virulent, potentially pandemic clone (Fig. 3c).

Our model posits that VAPs are circulating in the environment prior to the acquisition of key virulence factors. This is based on experimental evidence that a current pandemic strain cannot efficiently colonize the mammalian intestine without a PG-like *ompU* allele. If virulence adaptive alleles of *ompU* are indeed required prior to the acquisition of virulence factors, we would expect the same phenotypes of PG-like and EG-like *ompU* alleles in the genomic background of a more deeply branching PG isolate, such as classical *V. cholerae*. Indeed, we found that PG-like *ompU* alleles in the classical O395 background conferred efficient host colonization (Supplementary Fig. 7), which is consistent with an *ompU* VAP having played a role in the emergence of pandemic *V. cholerae*.

Our model further postulates that virulence adaptive alleles become enriched in the environmental population. Such enrichment would be made possible if these alleles provided a selective advantage in a newly available ecological niche, such as a human population consuming brackish water[28]. In previous work, we modeled an evolving, recombining microbial population that encounters a new ecological opportunity[29]. When adaptation to the new niche depends on few loci under positive selection in the niche, it is more likely for recombination to assemble the right combination of alleles in the same genome. These loci (akin to VAPs) could

contribute additively or synergistically to fitness. For example, the PG-like *ompU* alleles confer a tenfold increase in fitness during host colonization (Fig. 2d). Other VAPs might contribute further to this enhancement in host colonization. As more loci are involved in adaptation, it becomes less likely to achieve the optimal combination. Assuming the *V. cholerae* population undergoes approximately 100 recombination events per locus per generation (6.5 recombination events for every point mutation)[19], equivalent to a recombination rate of 10^{-4} in the modelled population of size 10^6, an optimal combination of alleles at five loci could conceivably evolve, but seven loci is very unlikely[29]. Therefore, if virulence depended on five or fewer positively selected loci in the *V. cholerae* genome, the optimal combination of alleles would be expected to appear repeatedly in nature. Given suitable ecological opportunities, it is then plausible that pandemic *V. cholerae* could emerge multiple times, originating from outside the PG group. However, the number of loci that are sufficient for the emergence of a virulent strain remains unknown and if it was much greater than five, pathogen emergence would be naturally limited. We identified eight candidate VAPs in our two datasets, and if all eight are phenotypically confirmed to be VAPs, this number of VAPs (>5) might naturally limit pandemic clone emergence. Furthermore, these eight candidate VAPs passed stringent filters and we suspect there might exist additional VAPs in the genome, identifiable by further sampling and experimentation.

Here we have described a framework for identifying loci that are present in a natural population and confer properties beneficial for virulence prior to acquisition of essential virulence genes and host colonization. This framework could be applied to other bacterial pathogens that emerge as clonal offshoots from non-virulent relatives, including *Yersinia, Salmonella, Escherichia*, or other pathogenic *Vibrio* species[1-4,6]. Pathogens that emerged through clonal expansion limit our ability to dissect the genetic basis of their pathogenicity, because bacterial genome-wide association studies lack power when the phenotype of interest has evolved only once[30]. Our framework therefore provides a way forward to identify the genetic

226 basis of virulence, even in pathogens that evolved through clonal expansion, and begin to

227 assess the risk of pathogen emergence and reemergence from environmental gene pools.

Methods

Genome sequencing. DNA from clinical isolates (Bgd1, Bgd5, Bgd8, MQ1795[31,32]) and environmental isolates (GBE0428, GBE0658, GBE1068, GBE1114, GBE1173[17]) was extracted using the Gentra kit (QIAGEN) and purified using the MoBio PowerClean Pro DNA Clean-Up Kit. Multiplexed genomic libraries were constructed using the Illumina-compatible Nextera DNA Sample Prep kit following the manufacturer's instructions. Sequencing was performed with 250-bp paired-end (v2 kit) reads on the illumina MiSeq.

Genome assembly. To exclude low-quality data, raw reads were filtered with Trimmomatic[33]. The 15 first bases of each reads were trimmed and reads containing at least one base with a quality score of <30 were removed. *De novo* assembly was performed on the resulting reads using Ray v2.3.1[34].

Genome alignment, annotation and SNP calling. We used mugsy v.1 r.2.2[35] with default parameters to align the primary dataset of 22 *V. cholerae* genomes (Supplementary Table 1). From this alignment, we extracted dimorphic SNP sites and annotated genes according to MJ-1236 as a reference genome. We defined the core genome as locally colinear blocks (LCBs) with all 22 genomes present in the alignment. We replicated the alignment, annotation and SNP calling using 21 different *V. cholerae* genomes, mainly from Orata *et al*.[18], plus the MJ-126 reference (Supplementary Table 1).

Definition of orthologous groups. Genomes were annotated using the RAST web server (www.rast.nmpdr.org)[36]. Annotated genes were clustered into orthologous groups using OrthoMCL (www.orthomcl.org)[37] with default parameters, yielding 2844 orthologous groups.

Phylogenetic analysis. We constructed a core genome phylogeny using the concatenated alignment of 1031 single-copy orthologous protein-coding genes (present in exactly one copy in each of the 22 primary dataset genomes). Each protein sequence was aligned with Muscle[38], and the concatenated alignment was used to infer an approximate maximum likelihood phylogeny with FastTree v. 2.1.8[39] using default parameters (Fig. 1a). Individual gene trees (Fig. 1d) were built in the same way. We constructed a neighbour-net of the 22 genomes using SplitsTree v.4.10[40], based on dimorphic SNPs from the mugsy genome alignment, excluding sites with gaps.

Tests for selection. We conducted a genome-wide version of the McDonald-Kreitman test[41] by first counting the number of fixed nonsynonymous (fn), fixed synonymous (fs), polymorphic nonsynonymous (pn), and polymorphic synonymous (ps) sites within each gene. We then summed these values across all genes (FN, FS, PN, and PS) and calculated the genome-wide Fixation Index, FI=(FN/FS)/(PN/PS). A fixation index greater than one suggests positive selection between the ingroup and outgroup (in this case, between EGs and PGs). However, care must be taken when computing a genome-wide FI because summing genes with different amounts of substitutions and polymorphism can result in FI>1 in the absence of selection[42]. We therefore performed 1000 permutations of the data, keeping the row totals (fn+fs and pn+ps) and column totals (fn+pn and fs+ps) constant and recomputing FI. We used the mean FI from the permutations as the expected value of FI under neutral evolution. To evaluate the hypothesis that the observed FI was higher than expected, suggesting positive selection, we computed a *P*-value as the fraction of permutations with FI greater or equal to the observed FI.

We repeated the test using polymorphism from either the PG group or the EG group (Supplementary Table 3).

To identify individual genes under selection between PGs and EGs in the primary dataset, we restricted our search to 87 genes with fn > 0.68 1 and fn:fs > 1.48 (respectively two standard deviations about the genome-wide medians). We then calculated the gene-specific FI and assessed its significance with a Fisher exact test. We found no genes with FI significantly greater than one, after Bonferroni correction for 87 tests. Similarly, in the replication dataset, we restricted our search to 26 genes with fn > 1.5 and fn:fs > 1.70, none of which had significantly high FI after correction for multiple tests.

To identify genes with an excess of nonsynonymous mixed SNPs (likely due to selection for amino acid changes), we restricted our search to five genes with ≥ 12 NS mixed SNPs per gene and mixed NS:S > 1.78 (respectively two standard deviations above the genome-wide medians). We used a one-sided binomial test to assess whether the observed NS:S ratio for each gene was significantly greater than the genome-wide median NS:S ratio of 0.5 (after adding a pseudocount of one to both NS and S). Three out of the five genes had a significantly high mixed NS:S ratio ($P < 0.05$) after Bonferroni correction for five tests (Table 1). We repeated this procedure in the replication dataset, identifying genes with ≥ 18 NS mixed SNPs per gene and mixed NS:S > 1.65 (respectively two standard deviations above the genome-wide medians). We used a one-sided binomial test to assess whether the observed NS:S ratio for

each gene was significantly greater than the genome-wide median NS:S ratio of 0.33 (after adding a pseudocount of one to both NS and S). The results of these tests are shown for genes also identified in the primary dataset (Table 1) and three additional genes identified in the replication dataset (Supplementary Table 5).

Bacterial strains and plasmids. *V. cholerae* O395 and *V. cholerae* N16961 were used as wild-type strains of classical and El Tor biotypes respectively. Strains cultivated on solid medium were grown on LB agar; strains in liquid media were grown in aerated LB broth at 37°C. pKAS154 was used for allelic exchange[43]. When necessary, media was supplemented with antibiotics to select for certain plasmids or strains of *V. cholerae* at the following concentrations: gentamycin, 30μg/ml; kanamycin, 45μg/ml; polymyxin B, 50μg/ml; and streptomycin, 1 mg/ml.

Strain construction. In-frame deletions and exchange of *ompU* alleles in both O395 and N16961 biotypes were constructed via homologous recombination[43]. For *ompU* deletions, PCR was used to amplify two 500 bp fragments flanking the *ompU* gene and to introduce restriction sites for cloning into the suicide vector pKAS154. For exchange of environmental *ompU* alleles, the respective allele was also amplified using the extracted DNA from each environmental strain. Restriction sites were introduced in the primers. The fragments were then cloned into a restriction-digested suicide plasmid, pKAS154, using a four-segment ligation for each environmental allele exchange mutants (plasmid, *ompU* flanking fragments and environmental *ompU* allele). The resulting plasmids were electroporated into *Escherichia coli* S17-1λpir. *E. coli* with the constructed inserts. Different sizes of *ompU* genes were confirmed, sequenced and

316 compared to the genome sequences of environmental strains. For both deletion and exchange
317 mutants, plasmids with the insert of interest were mated with wild-type *V. cholerae* O395 or
318 N16961, and allelic exchange was carried out by selection on antibiotics as described
319 previously[43]. For a more detailed description of allelic exchange please refer to Skorupski and
320 Taylor 1998[43]. Potential mutants were screened using PCR: two primers flanking the deletion
321 construct were used to amplify chromosomal DNA isolated from plated *V. cholerae*. The lengths
322 of the PCR fragments were analyzed on 0.8% agarose gel for gene deletions and putative
323 deletions and allele exchange were subsequently confirmed by DNA sequencing.
324
325 **OmpU visualization and immunobloting.** Whole cell protein extracts were prepared from
326 cultures grown for overnight at 37°C in a rotary shaker. The extracts were subjected to SDS-
327 PAGE on 16% Tris Glycine gels (Invitrogen). OmpU bands were visualized after protein gels
328 were stained by Coomassie blue overnight. Prior to staining the gels were transferred to
329 nitrocellulose membranes using iBlot (Invitrogen). The membranes were blocked O/N in Tris-
330 Buffered Saline, 3% BSA. Primary OmpU antibodies were diluted 1:10,000 in TBST (Tris-
331 Buffered Saline, 0.5% Tween-20). Membranes were incubated with primary antibodies for 2
332 hours at room temperature. After incubation, the membranes were washed with TBST four
333 times. Goat anti-rabbit secondary antibodies (BioRad) were diluted 1:10,000 in TBST and
334 incubated for 30 minutes at room temperature. The membranes were washed 4 times with TBS
335 (Tris-Buffered Saline). Reactive protein bands were detected via ECL (Amersham).
336
337 **Survival assays.** *V. cholerae* strains were cultured overnight in LB broth at 37°C in a rotary
338 shaker. Overnight cultures were diluted 1:100 in LB and grown to an OD600 of 0.5. Cells were

339 pelleted and resuspended in either LB broth, LB containing 0.4% bile bovine (Sigma), or LB
340 containing 1000U/ml of polymyxin B (Sigma). Cultures were incubated for 1h at 37°C in a rotary
341 shaker. After incubation CFU/ml of each culture was calculated by plating dilutions in LB plates.
342 Survival was calculated by comparing the number of CFU/ml in LB plus treatment versus LB.
343 N≥6. No samples were excluded.
344
345 **Infant mouse competition assays.** Overnight cultures were diluted 1:100. Each test strain was
346 mixed in a 1:1 ratio with a Δ*lacZ* reference strain. Four- to five-day-old CD-1 mice (*Mus*
347 *musculus*) from several mixed litters were randomly inoculated orogastrically in blinded
348 experiments with 50µl of the bacterial mixture. Sex of the animals was not inspected prior to
349 inoculations. The intestines were harvested 24h post-inoculation and homogenized in 4ml of LB
350 broth containing 10% glycerol. The mixtures were serially diluted and plated on LB agar plates
351 supplemented with streptomycin and 5-bromo-4-chloro-3-indolyl-D-galactopyramoside (X-Gal)
352 (40µg/ml). The competition indices were calculated as previously described by others, test
353 (output CFUs/input CFUs)/reference (output CFUs/ input CFUs) and the sample size selected
354 was appropriate for statistical analysis. No samples or animals were excluded. Animal work was
355 approved by the Institutional Animal Care and Use Committee (IACUC).
356
357 **Biofilm assays.** 96-well plate assay. Cultures were incubated overnight at 30°C. 100µl of 1:100
358 dilutions of overnight cultures were placed per well in 96-well plates. Plates were left at 25°C for
359 24h. Liquid contents were discarded and plates were washed 2 times with LB. 200µl of 0.01%

crystal violet was added per well and incubated at room temperature for 5 minutes. Liquid contents were discarded and plates were washed extensively with dH_2O. After the plates were dry, biofilms were resuspended in 150µl of 50% acetic acid. Contents were transferred to a flat bottom dish and quantitated in a microtiter plate reader at OD550. Values were plotted using Prism software. N=15.

Data availability

The nine genomes sequenced in this study (Bgd1, Bgd5, Bgd8, MQ1795, GBE0428, GBE0658, GBE1068, GBE1114, GBE1173) have been deposited under BioProject ID PRJNA349157 in NCBI GenBank under accession numbers SAMN05924900-SAMN05924908 (Supplementary Table 1). All other data supporting the findings of this study are available from the authors upon request.

References

1. McNally, A., Thomson, N. R., Reuter, S. & Wren, B. W. 'Add, stir and reduce': Yersinia spp. as model bacteria for pathogen evolution. *Nat. Rev. Microbiol.* **14,** 177–190 (2016).
2. Luo, C. *et al.* Genome sequencing of environmental *Escherichia coli* expands understanding of the ecology and speciation of the model bacterial species. *Proc. Natl. Acad. Sci. U.S.A.* **108,** 7200–7205 (2011).
3. Reen, F. J., Almagro-Moreno, S., Ussery, D. & Boyd, E. F. The genomic code: inferring Vibrionaceae niche specialization. *Nat. Rev. Microbiol.* **4,** 697–704 (2006).
4. Ochman, H. Genes Lost and Genes Found: Evolution of Bacterial Pathogenesis and Symbiosis. *Science* **292,** 1096–1099 (2001).
5. Shapiro, B. J. How clonal are bacteria over time? *Curr. Opin. Microbiol.* **31,** 116–123 (2016).
6. Cui, Y. *et al.* Epidemic Clones, Oceanic Gene Pools, and Eco-LD in the Free Living Marine Pathogen *Vibrio parahaemolyticus. Mol. Biol. Evol.* **32,** 1396–1410 (2015).
7. Chun, J. *et al.* Comparative genomics reveals mechanism for short-term and long-term clonal transitions in pandemic *Vibrio cholerae*. *Proc. Natl. Acad. Sci. U.S.A.* **106,** 15442–15447 (2009).
8. Boucher, Y. Sustained local diversity of *Vibrio cholerae* O1 biotypes in a previously cholera-Free country. *mBio* **7,** e00570–16 (2016).
9. Mutreja, A. *et al.* Evidence for several waves of global transmission in the seventh cholera pandemic. *Nature* **477,** 462–465 (2011).
10. Taylor, R. K., Miller, V. L., Furlong, D. B. & Mekalanos, J. J. Use of phoA gene fusions to identify a pilus colonization factor coordinately regulated with cholera toxin. *Proc. Natl. Acad. Sci. U.S.A.* **84,** 2833–2837 (1987).
11. Waldor, M. K. & Mekalanos, J. J. Lysogenic conversion by a filamentous phage encoding cholera toxin. *Science (New York, N.Y.)* **272,** 1910–1914 (1996).
12. Karaolis, D. K. *et al.* A *Vibrio cholerae* pathogenicity island associated with epidemic and pandemic strains. *Proc. Natl. Acad. Sci. U.S.A.* **95,** 3134–3139 (1998).
13. Faruque, S. M. *et al.* Genetic diversity and virulence potential of environmental *Vibrio cholerae* population in a cholera-endemic area. *Proc. Natl. Acad. Sci. U.S.A.* **101,** 2123–2128 (2004).
14. Rivera, I. N., Chun, J., Huq, A., Sack, R. B. & Colwell, R. R. Genotypes associated with virulence in environmental isolates of *Vibrio cholerae. Appl. Environ. Microbiol.* **67,** 2421–2429 (2001).
15. Gennari, M., Ghidini, V. & Lleo, M. M. Virulence genes and pathogenicity islands in environmental Vibrio strains non-pathogenic to humans. *FEMS Microbiol. Ecol.* **82,** 563–573 (2012).
16. Dziejman, M. *et al.* Genomic characterization of non-O1, non-O139 *Vibrio cholerae* reveals genes for a type III secretion system. *Proc. Natl. Acad. Sci. U.S.A.* **102,** 3465–3470 (2005).
17. Schuster, B. M. *et al.* Ecology and genetic structure of a northern temperate *Vibrio cholerae* population related to toxigenic isolates. *Appl. Environ. Microbiol.* **77,** 7568–7575 (2011).
18. Orata, F. D. *et al.* The dynamics of genetic interactions between *Vibrio metoecus* and *Vibrio cholerae*, two close relatives co-occurring in the environment. *Genome Biol Evol* **7,** 2941–2954 (2015).
19. Keymer, D. P. & Boehm, A. B. Recombination shapes the structure of an environmental *Vibrio cholerae* population. *Appl. Environ. Microbiol.* **77,** 537–544 (2011).
20. Provenzano, D., Schuhmacher, D. A., Barker, J. L. & Klose, K. E. The virulence regulatory protein ToxR mediates enhanced bile resistance in *Vibrio cholerae* and other pathogenic Vibrio species. *Infect. Immun.* **68,** 1491–1497 (2000).
21. Mathur, J. & Waldor, M. K. The *Vibrio cholerae* ToxR-regulated porin OmpU confers resistance to antimicrobial peptides. *Infect. Immun.* **72,** 3577–3583 (2004).
22. Almagro-Moreno, S., Pruss, K. & Taylor, R. K. Intestinal colonization dynamics of *Vibrio cholerae*. *PLoS Pathog.* **11,** e1004787 (2015).
23. Merrell, D. S., Bailey, C., Kaper, J. B. & Camilli, A. The ToxR-mediated organic acid tolerance response of *Vibrio cholerae* requires OmpU. *J. Bacteriol.* **183,** 2746–2754 (2001).
24. Watnick, P. I. & Kolter, R. Steps in the development of a *Vibrio cholerae* El Tor biofilm. *Mol. Microbiol.* **34,** 586–595 (1999).
25. Valeru, S. P., Wai, S. N., Saeed, A., Sandström, G. & Abd, H. ToxR of *Vibrio cholerae* affects biofilm, rugosity and survival with *Acanthamoeba castellanii*. *BMC Res Notes* **5,** 33 (2012).
26. Yildiz, F. H. & Schoolnik, G. K. *Vibrio cholerae* O1 El Tor: identification of a gene cluster required for the rugose colony type, exopolysaccharide production, chlorine resistance, and biofilm formation. *Proc. Natl. Acad. Sci. U.S.A.* **96,** 4028–4033 (1999).

27. Hsiao, A., Liu, Z., Joelsson, A. & Zhu, J. *Vibrio cholerae* virulence regulator-coordinated evasion of host immunity. *Proc. Natl. Acad. Sci. U.S.A.* **103,** 14542–14547 (2006).
28. Boucher, Y., Orata, F. D. & Alam, M. The out-of-the-delta hypothesis: dense human populations in low-lying river deltas served as agents for the evolution of a deadly pathogen. *Front. Microbiol.* **6,** L19401 (2015).
29. Friedman, J., Alm, E. J. & Shapiro, B. J. Sympatric Speciation: When Is It Possible in Bacteria? *PLoS ONE* **8,** e53539 (2013).
30. Chen, P. E. & Shapiro, B. J. The advent of genome-wide association studies for bacteria. *Curr. Opin. Microbiol.* **25,** 17–24 (2015).
31. Nair, G. B. *et al.* New variants of *Vibrio cholerae* O1 biotype El Tor with attributes of the classical biotype from hospitalized patients with acute diarrhea in Bangladesh. *J. Clin. Microbiol.* **40,** 3296–3299 (2002).
32. Son, M. S., Megli, C. J., Kovacikova, G., Qadri, F. & Taylor, R. K. Characterization of *Vibrio cholerae* O1 El Tor biotype variant clinical isolates from Bangladesh and Haiti, including a molecular genetic analysis of virulence genes. *J. Clin. Microbiol.* **49,** 3739–3749 (2011).
33. Bolger, A. M., Lohse, M. & Usadel, B. Trimmomatic: a flexible trimmer for Illumina sequence data. *Bioinformatics* **30,** 2114–2120 (2014).
34. Boisvert, S., Raymond, F., Godzaridis, É., Laviolette, F. & Corbeil, J. Ray Meta: scalable de novo metagenome assembly and profiling. *Genome Biol* **13,** R122 (2012).
35. Samuel V Angiuoli, S. L. S. Mugsy: fast multiple alignment of closely related whole genomes. *Bioinformatics* **27,** 334–342 (2011).
36. Aziz, R. K. *et al.* The RAST Server: Rapid Annotations using Subsystems Technology. *BMC Genomics* **9,** 1 (2008).
37. Li, L., Stoeckert, C. J. & Roos, D. S. OrthoMCL: identification of ortholog groups for eukaryotic genomes. *Genome Res.* **13,** 2178–2189 (2003).
38. Edgar, R. C. MUSCLE: multiple sequence alignment with high accuracy and high throughput. *Nucleic Acids Res.* **32,** 1792–1797 (2004).
39. Price, M. N., Dehal, P. S. & Arkin, A. P. FastTree 2 – Approximately Maximum-Likelihood Trees for Large Alignments. *PLoS ONE* **5,** e9490 (2010).
40. Bryant, D. & Moulton, V. Neighbor-net: an agglomerative method for the construction of phylogenetic networks. *Mol. Biol. Evol.* **21,** 255–265 (2004).
41. McDonald, J. H. & Kreitman, M. Adaptive protein evolution at the Adh locus in Drosophila. *Nature* **351,** 652–654 (1991).
42. Shapiro, J. A. *et al.* Adaptive genic evolution in the Drosophila genomes. *Proc. Natl. Acad. Sci. U.S.A.* **104,** 2271–2276 (2007).
43. Skorupski, K. & Taylor, R. K. Positive selection vectors for allelic exchange. *Gene* **169,** 47–52 (1996).

Correspondence should be addressed to:

Salvador Almagro-Moreno (samoreno@ucf.edu)

Acknowledgements

The authors would like to thank the anonymous reviewers for their thoughtful comments and suggestions. We would also like to thank Otto Cordero, Yves Terrat, Nicolas Tromas and Britney Privett for constructive comments on the manuscript. We thank Lawrence Shelven for his highly valuable technical assistance. BJS was supported by a Canada Research Chair and the Canadian Institutes for Health Research. RKT was supported by a National Institutes of Health grants AI039654 and AI025096. SAM was supported by startup funds from the Burnett School of Biomedical Sciences at the University of Central Florida and Dartmouth College's E. E. Just Postdoctoral Fellowship. This article is dedicated to the memory of Ronald K. Taylor.

Author contributions

SAM conceived the study. BJS, RKT and SAM designed the study. IL sequenced genomes. BJS performed computational analysis. GK and SAM performed phenotypic characterization. BJS and SAM analyzed, interpreted data and wrote the article. All authors have read a version of the manuscript.

Figure Legends

Figure 1. Comparative genomics reveals candidate virulence adaptive polymorphisms. a, Phylogeny of 22 *V. cholerae* genomes based on 1031 single-copy orthologs in the primary dataset. All branches have local support values >0.99 (based on FastTree's approximate likelihood ratio test) except for very short, deep internal branches (resulting in the star-like polytomy at the centre of the tree). Not all 22 genomes are visible because some have nearly identical sequences (*e.g.* 6 of the 7 PG genomes are nearly identical, shown as an orange triangle; GBE1173 and GBE1114 are nearly identical, as can be seen in Supplementary Fig. 1). **b,** Distribution of fixed SNPs across chromosome 1. (See Supplementary Fig. 3 for chromosome 2). Genome position is according to the MJ-1236 reference genome. SNP-free regions (*e.g.* near 3 Mbp, the locus of the integrative conjugative element) are part of the flexible genome, present in the reference but not the other 21 genomes. The schematic tree in the top left illustrates the fixed SNP pattern, in which one allele is present in PGs and a different allele in EGs. **c**, Distribution of mixed SNPs across the genome. The cartoon tree in the top left illustrates the mixed SNP pattern, in which one allele is fixed in PGs, and another allele is polymorphic among EGs, with some EGs containing the PG-like allele. Black arrows show candidate VAPs (Table 1). Grey arrow shows the flagellum as an example variable region not containing candidate VAPs. **d**, *ompU* phylogeny. All visible branches have local support values >0.9 except for the branch separating RC385 and GBE0658, the branch grouping MJ-1236 and O395 together, and the branch grouping HE09 and VL426 together.

Figure 2. Phenotypic characterization of *ompU* alleles. a, OmpU production in clinical strains of *V. cholerae* encoding environmental alleles of *ompU*. Total protein lysates were run on a 16% Tris-glycine gel. OmpU bands were visualized after protein gels were stained with Coomassie

blue. Three independent sets of protein lysates were examined and showed an identical band pattern. **b**, Survival of *ompU* mutants in the presence of bile (n=7) or **c**, polymyxin B (n=6). **d**, Colonization of the small intestine of *ompU* mutant strains (n=6). **e**, Biofilm formation of *ompU* mutant strains on an abiotic surface (n=15). Yellow bars and symbols, PG-like allele; red bars and squares, Δ*ompU*; blue bars and triangles, EG-like allele. Center values represent the mean and error bars the standard deviation. Variance between the groups was similar. Statistical comparisons were made using Student's *t*-test. **P* < 0.05, ****P* < 0.001

Figure 3. Model of pandemic clone emergence from an environmental gene pool. We propose a model that involves three events required for the emergence of pathogenic clones from environmental populations. **a**, selection of VAPs. Virulence adaptive alleles circulate in naturally occurring populations (orange symbols) and can be exchanged and mobilized through recombination (green dashed arrows). Ecological variation (*e.g.* temperature, nutrient availability, pH, etc.) leads to the selection of VAPs and an increase in their distribution in environmental populations. **b**, enrichment of clones. A new ecological opportunity occurs (human consumption of untreated waters, transient colonization of new environmental hosts, etc.) which leads to the proliferation and enrichment in the population of clones encoding a mosaic of VAPs. **c**, acquisition of virulence factors**.** A strain encoding a minimum set of VAPs required for host colonization acquires the virulence factors that are necessary to produce a successful infection and give rise to pandemic disease.

Tables

Table 1. Characteristics of five predicted VAPs with an excess of nonsynonymous mixed SNPs.

	Gene ID (VCD #)	Annotation	Gene length (bp)	Total # SNPs	Mixed *dN*	Mixed *dS*	Mixed *dN/dS*	Mixed NS	Mixed S	*P*
1	003778	outer membrane protein OmpU	1053	204 (110)	0.037 (0.018)	0.045 (0.033)	0.83 (0.53)	28 (13)	11 (8)	0.0047* (0.0068*)
2	001600	hypothetical	258	21 (26)	0.082 (0.12)	0.081 (0.065)	1.01 (1.82)	15 (22)	4 (3)	0.0096* (2.32e-8*)
3	001013	hypothetical	642	19 (13)	0.034 (0.006)	0.029 (0.012)	1.18 (0.55)	15 (2)	4 (1)	0.0096* (n.s.)
4	001209	MSHA biogenesis protein MshP	432	85 (63)	0.047 (0.025)	0.045 (0.054)	1.04 (0.46)	14 (7)	4 (5)	0.0154 (0.066)
5	001230	lipid A core O-antigen ligase	1794	75 (47)	0.0098 (0.001)	0.013 (0.004)	0.76 (0.18)	12 (0)	5 (1)	0.0717 (n.s.)

NS=nonsynonymous; S=synonymous. *dN* = number of nonsynonymous SNPs per nonsynonymous site; *dS* = number of synonymous SNPs per synonymous site. Mixed SNPs are polymorphic in EGs but fixed in PGs, meaning that at least one EG contains a PG-like allele. The genes listed have mixed NS, mixed NS:S, and mixed *dN/dS* each over two standard deviations above their respective genome-wide medians in the primary dataset. A one-sided binomial test determined if the mixed NS:S ratio was greater than the expected genome-wide median value of 0.5 per gene (uncorrected *P*-values shown; asterisks (*) indicate $P < 0.05$ after Bonferroni correction for five tests). Numbers in parentheses are for the replication dataset, with an expected genome-wide median mixed N:S of 0.33. *P*-values greater than 0.1 are denoted as not significant (n.s.). Genes 1, 2, 4, and 5 are indicated with arrows on Figure 1C. Gene 3 is on chromosome 2 (Supplementary Fig. 3).

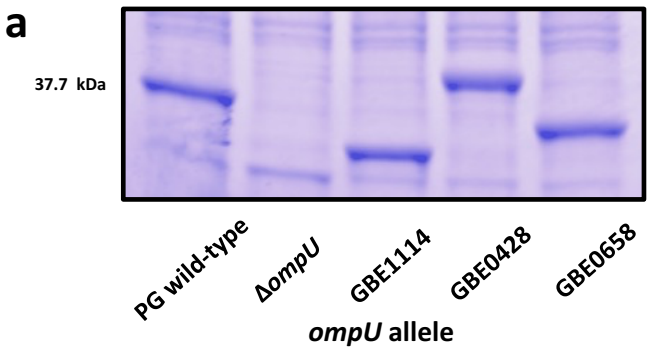

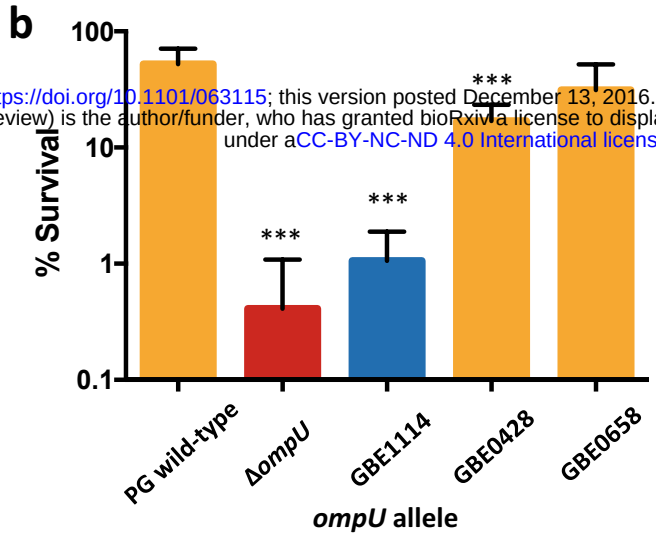

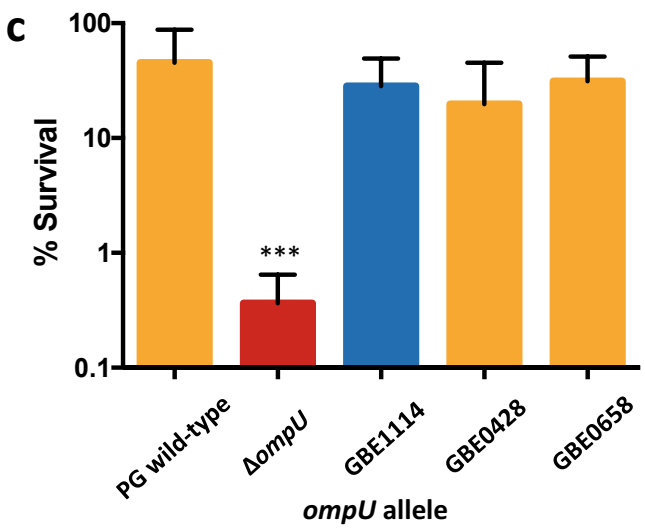

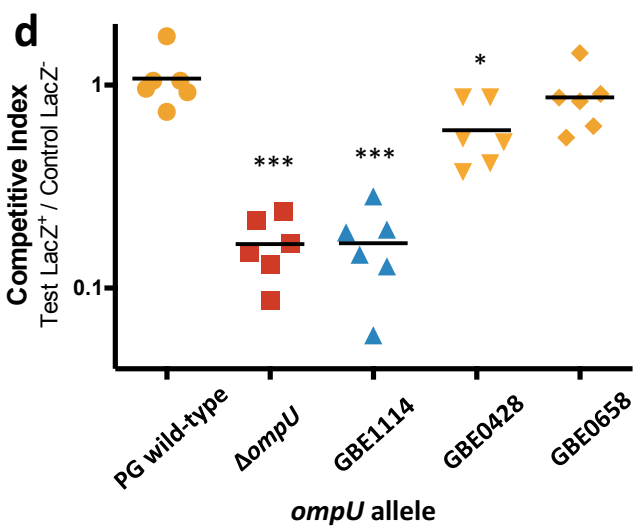

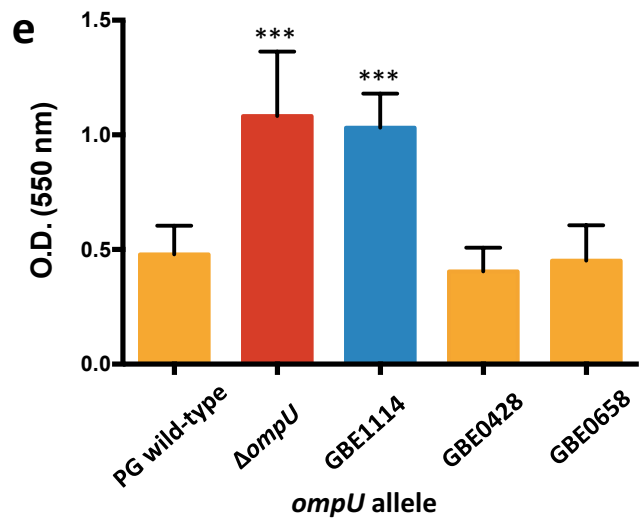

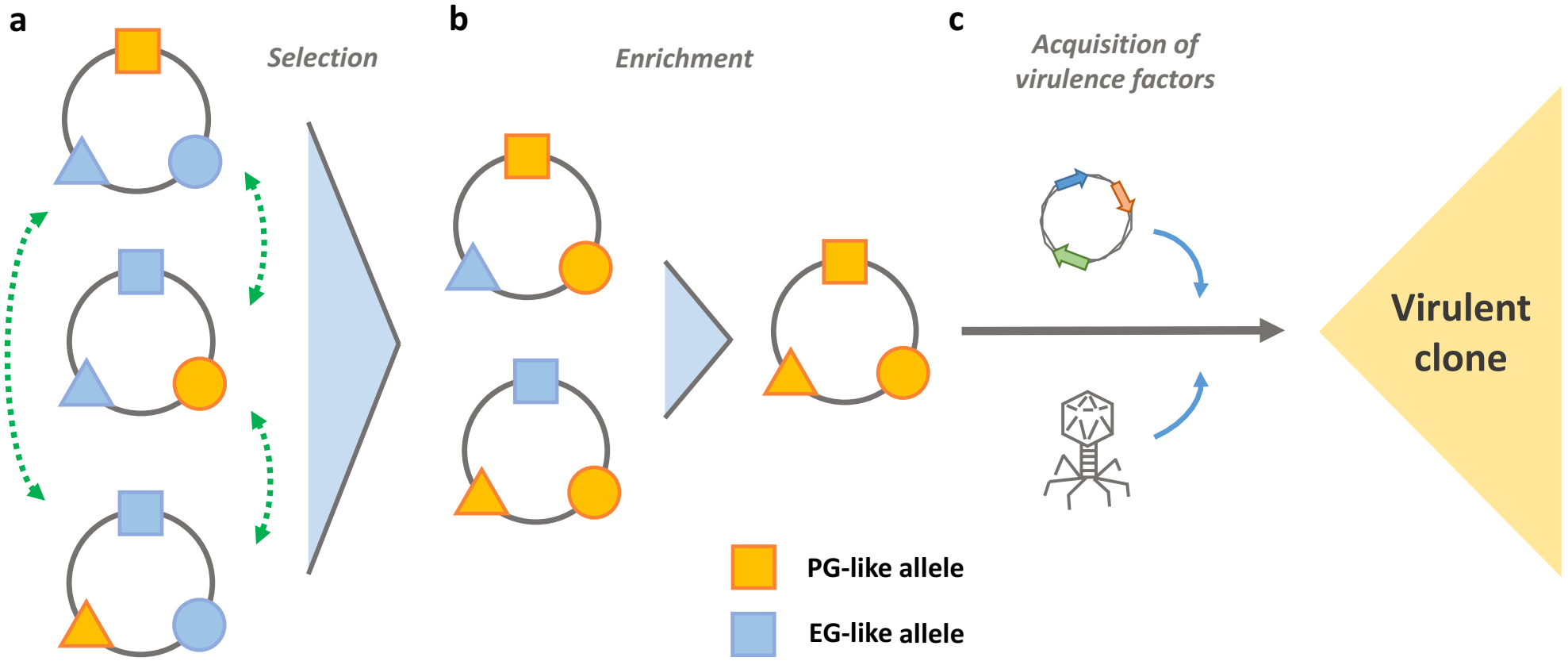
a
Selection
b
Enrichment
c
Acquisition of virulence factors
Virulent clone
PG-like allele
EG-like allele